ACS Energy LETTERS

http://pubs.acs.org/journal/aelccp

LETTER

Enhancing the Capacitive Performance of Electric Double-Layer Capacitors with Ionic Liquid Mixtures

C. Lian,[†,‡] K. Liu,[†] K. L. Van Aken,[§] Y. Gogotsi,[§] D. J. Wesolowski,[∥] H. L. Liu,[‡] D. E. Jiang,[⊥] and J. Z. Wu*[,†]

[†]Department of Chemical and Environmental Engineering, University of California, Riverside, California 92521, United States

[‡]State Key Laboratory of Chemical Engineering, East China University of Science and Technology, Shanghai 200237, P. R. China

[§]Department of Materials Science and Engineering and A.J. Drexel Nanomaterials Institute, Drexel University, Philadelphia, Pennsylvania 19104, United States

[∥]Chemical Sciences Division, Oak Ridge National Laboratory, Oak Ridge, Tennessee 37831, United States

[⊥]Department of Chemistry, University of California, Riverside, California 92521, United States

Supporting Information

ABSTRACT: Formulating room-temperature ionic liquid (RTIL) mixed electrolytes was recently proposed as an effective and convenient strategy to increase the capacitive performance of electrochemical capacitors. Here we investigate the electrical double-layer (EDL) structure and the capacitance of two RTILs, 1-ethyl-3-methylimidazolium bis(trifluoromethylsulfonyl)imide (EMI-TFSI) and 1-ethyl-3-methylimidazolium tetrafluoroborate (EMI-BF_4), and their mixtures with onion-like carbon electrodes using experiment and classical density functional theory. The principal difference between these ionic liquids is the smaller diameter of the BF_4^- anion relative to the $TFSI^-$ anion and the EMI^+ cation. A volcano-shaped trend is identified for the capacitance versus the composition of the RTIL mixture. The mixture effect, which makes more counterions pack on and more co-ions leave from the electrode surface, leads to an increase of the counterion density within the EDL and thus a larger capacitance. These theoretical predictions are in good agreement with our experimental observations and offer guidance for designing RTIL mixtures for EDL supercapacitors.

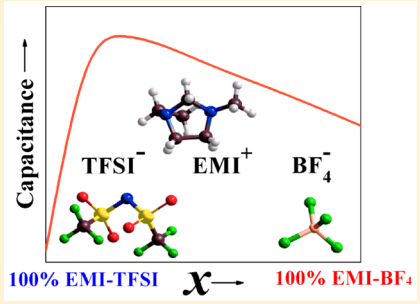

Electric double-layer capacitors (EDLCs), also known as supercapacitors, store electrical energy by physisorption of ionic species at the surface of porous electrodes. In comparison to electrochemical batteries, EDLCs have the advantages of faster charging kinetics, higher power densities, and longer cycling lifespans.[1] While surface reactions play a central role in batteries, the performance of supercapacitors is strongly correlated with the nonredox ionic behavior inside the micropores of electrodes.[2−7] The energy density per surface area of an EDLC is proportional to its capacity and to the square of its operating potential window (OPW), $E = CV^2/2$, where C is the capacitance per surface area and V the maximum OPW.[8−10] Accordingly, the energy density of an EDLC can be enhanced by increasing the specific surface area of the porous electrode, by maximizing the capacitance of the electric double layer (EDL), and by using electrolytes with a larger OPW.

Recently, a wide variety of carbon-based electrodes with diverse pore size distributions, morphology, architecture, and functionality have been utilized for EDLCs to improve the capacitive performance.[11−15] Among various electrolytes for EDLCs, organic electrolytes (e.g., propylene carbonate and acetonitrile) and room-temperature ionic liquids (RTILs) are preferred over conventional aqueous electrolytes in terms of their wider OPWs. In particular, ionic liquids are often adopted because of their large electrochemical windows, excellent thermal stability, and nonvolatility.[16] Because cations and anions of the RTILs typically have different electrochemical stability, the maximum working potentials of the negative and positive electrodes are asymmetric, and such asymmetry can also affect the OPW of an EDLC. To utilize the entire working potential ranges, one may take a variety of approaches including charge injection,[17] mass balancing,[18] and asymmetric carbon selection.[19] However, all these methods have negative side effects on the EDLC performance. Recently, some of us proposed an alternative yet much simpler strategy: using ionic liquid mixtures to balance the electrode's performance during charging and discharging, thereby increasing the range of the

Received: March 9, 2016
Accepted: April 11, 2016
Published: April 18, 2016

DOI: 10.1021/acsenergylett.6b00010
ACS Energy Lett. 2016, 1, 21−26

operating potential.[20] While the adoption of ionic mixtures is promising, the origin of such mixture effect is still unclear.

Despite a large amount of theoretical and simulation work on the capacitance of RTILs in porous electrodes,[6,21−31] little is known about how the properties of EDLCs containing RTIL mixtures would be affected by the electrolyte composition.[32−35] Toward the rational design of the electrolytes and electrode materials, it would be desirable to understand the following: How would the EDL structure and capacitance change with the composition of RTIL mixtures? What is the microscopic mechanism underlying the capacitance change? Importantly, what is the functional role of individual ions in the EDL behavior? To address these questions, we employ classical density functional theory (CDFT) to study the properties of EDLs of RTIL mixtures near the electrodes. CDFT is an ideal computational tool for examining the mixture effects because it is computationally efficient and applicable to a wide variety of systems ranging from electrodes with pore size comparable to the ionic dimensionality to those with pores on the mesoscopic scales.

As in previous work,[25,36] we use the primitive model of electrolytes to represent RTILs. Whereas the coarse-grained model lacks chemical specificities, it accounts for electrostatic correlations and ionic excluded volume effects that are ignored in conventional electrochemical theories (e.g., the Poisson−Boltzmann equation). Both effects are important for describing the performance of RTIL-based EDLCs. Figure 1 shows a

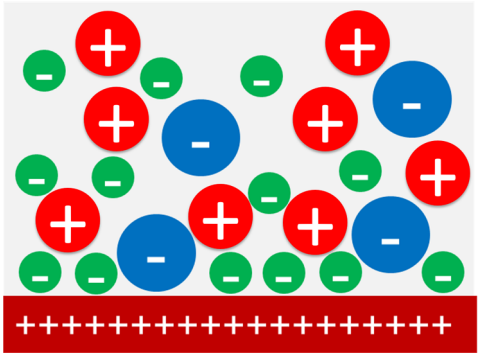

Figure 1. Schematic representation of a RTIL mixture near the electrode surface. In the coarse-grained model, cations and anions are represented as charged hard spheres of different diameters and the electrode surface has a planar geometry.

schematic representation of our model ionic system. Here, cations and anions are charged hard spheres, and the electrode is represented by a planar surface. The pair potential between the ionic species is given by

$$u_{ij}(r) = \begin{cases} \infty, & r < (\sigma_i + \sigma_j)/2 \\ Z_i Z_j e^2/4\pi\varepsilon_0 r, & r \geq (\sigma_i + \sigma_j)/2 \end{cases} \quad (1)$$

where r is the center-to-center distance, e the elementary charge, and ε_0 the permittivity of the free space; σ_i and Z_i are the diameter and the valence of particle i, respectively. Following previous publications,[25,36] we select the model parameters (viz. hard-sphere diameters and ionic valences) by matching the molecular volumes and the charges of ionic species in 1-ethyl-3-methylimidazolium bis(trifluoromethylsulfonyl)imide (EMI-TFSI) and 1-ethyl-3-methylimidazolium tetrafluoroborate (EMI-BF_4), two commercial ionic liquids widely used in electrochemical devices.[1] Throughout this work, both anions and cations are assumed monovalent ($Z_i = -1$ and $+1$) as is the case for EMI^+, $TFSI^-$, and BF_4^-. The diameter of cations (EMI^+) is fixed at $\sigma_+ = 0.5$ nm, and the diameters of anions are 0.6 and 0.3 nm for $TFSI^-$ and BF_4^-, respectively. The effective diameters were estimated from their molecular volumes optimized by Dmol[3] module of Materials Studio version 7.0.[37] For all mixtures, the total number density is 2.32 nm^{-3} for both cations and anions, and the overall charge neutrality is imposed for the entire electrochemical cell.[38]

As in standard EDL theories, the electrode is modeled as a rigid planar wall. The model is a simplification of the external surface of an onion-like carbon (OLC) electrode, as was used in the experimental investigation of RTIL mixture effects.[20] The OLC particles have a spherical shape with a diameter between 5 and 10 nm and are free of micropores.[20,39,40] It has been shown with molecular dynamics simulation that the curvature effect on the OLC-EDLCs is relatively insignificant when the particle size is beyond several nanometers.[41] Therefore, the planar model mimics the OLC-EDLCs studied experimentally. The charged wall exerts an external potential on each ion given by

$$V_i(z) = \begin{cases} \infty, & z < \dfrac{\sigma_i}{2} \\ -2\pi Z_i e Q z/\varepsilon_0, & z \geq \dfrac{\sigma_i}{2} \end{cases} \quad (2)$$

where Q stands for the surface charge density and z is the perpendicular distance.

We calculate the ion distributions and subsequently the capacitance using CDFT.[42] At a given temperature, T, and a set of ion concentrations in the bulk, ρ_i^0, CDFT predicts the ion distributions near the electrode surface

$$\rho_i(z) = \rho_i^0 \exp[-\beta V_i(z) - \beta Z_i e\psi(z) - \beta\Delta\mu_i^{ex}(z)] \quad (3)$$

where $\beta = 1/(k_B T)$ and k_B is the Boltzmann constant; $\Delta\mu_i^{ex}(z)$ accounts for electrostatic correlations and ionic excluded volume effects.[42] The electrical potential, $\psi(z)$, is related to the local charge density by the Poisson equation

$$\frac{\partial^2\psi(z)}{\partial z^2} = -\frac{e}{\varepsilon_0\varepsilon_{bulk}}\sum_i Z_i\rho_i(z) \quad (4)$$

Without $\Delta\mu_i^{ex}(z)$, eqs 3 and 4 reduce to the conventional Poisson−Boltzmann equations.

The analytical expression for $\Delta\mu_i^{ex}(z)$ and numerical details for CDFT calculations have been reported in our previous work.[36] Briefly, eqs 3 and 4 are solved self-consistently with the boundary conditions for the electrical potential

$$\psi(0) = \psi;\ \psi(\infty) = 0 \quad (5)$$

In the CDFT calculations, the electric potential at the electrode surface, ψ, is assumed to be constant. The charge density, Q, is calculated from the condition of overall charge neutrality. To solve eqs 3 and 4, we start with an initial guess for the ionic density profiles, $\rho_i(z)$. The local excess chemical potential for each ionic species and the local electrical potential, $\Delta\mu_i^{ex}(z)$ and $\psi(z)$, are then calculated from the ionic density profiles. Next, a new set of ionic density profiles are obtained from eq 3, and the procedure repeats until convergence ($|\Delta\rho_i/\rho_i^0| < 10^{-4}$ at all positions). Once we have the ion distributions and the electrical potential profiles, we calculate the surface charge density (Q) and the integral capacitances from

DOI: 10.1021/acsenergylett.6b00010
ACS Energy Lett. 2016, 1, 21−26

$$Q = -\sum_i Z_i e \int_0^\infty dz\, \rho_i(z) \tag{6}$$

and

$$C = Q/(\psi - \mathrm{PZC}) \tag{7}$$

where PZC stands for the potential of zero charge.

In parallel to the theoretical investigations, we performed an experiment on the effects of ionic composition on the capacitance of OLC-EDLCs. As in previous work,[20,40,43] a symmetric supercapacitor device was tested with two identical OLC electrodes in a traditional sandwich setup. The electrodes were ∼100 μm thick and 12 mm in diameter, and their weight was in the range of 9−10 mg of OLC per electrode. Electrochemical characterization was performed on a VMP3 potentiostat/galvanostat (Bio-Logic) using cyclic voltammetry to measure the performance. The capacitance is calculated from

$$C = \frac{2}{Vm} \int I(t)\, dt \tag{8}$$

where C is the electrode capacitance (F/g), $I(t)\,dt$ the discharge current as a function of time (As), V the operating voltage window (V), and m the mass of a single electrode (g). For more experimental details, we refer the reader to ref 20.

To illustrate the mixture effects on EDL performance, we consider first the ion distributions and surface charge densities for EMI-TFSI-BF_4 mixtures at various electric potentials. Figure 2 shows the CDFT predictions for the surface charge density

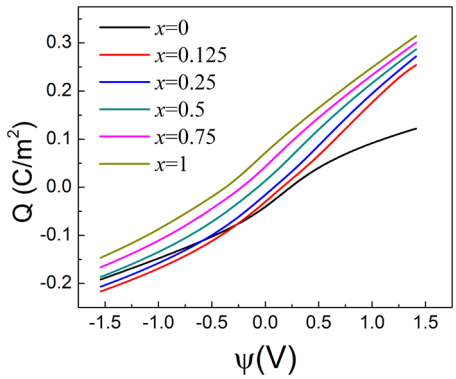

Figure 2. Charge density as a function of the electrode potential at several compositions of the EMI-TFSI-BF_4 mixture. Here, x represents the mole fraction of EMI-BF_4 in the RTIL mixture; x = 0 means pure EMI-TFSI, while x = 1 is for pure EMI-BF_4.

versus the electrode potential for different mole fractions of EMI-BF_4, x. While the surface charge density rises monotonically with the electrode potential, we observe a notable change of the curvature at various EMI-BF_4 contents. Different from previous studies of symmetric ionic systems (cations and anions have the same size and absolute valence),[4,36,38] the Q−ψ curves are noticeably asymmetric for RTIL mixtures. Interestingly, the potential of zero charge (PZCs) for pure EMI-TFSI and pure EMI-BF_4 are positive and negative, respectively. The sign of the PZC can be explained in terms of the asymmetry between the diameters of cations and anions, i.e., near a neutral electrode larger ions are distributed closer to the surface than smaller ions. Increasing the composition of EMI-BF_4 in the RTIL mixture shifts the PZC from slightly positive to neutral or negative. For the positive electrode, introduction of EMI-BF_4 to EMI-TFSI results in a dramatic increase of the surface charge density due to smaller (BF_4^-) anions accumulated near the positively charged surface.

We now consider how the EDLC capacitance changes with the content of the smaller anions at the same applied potential. Here, the voltages of cathode and anode are fixed at 1.5 and −1.5 V, respectively. Figure 3a presents the integral capacitance

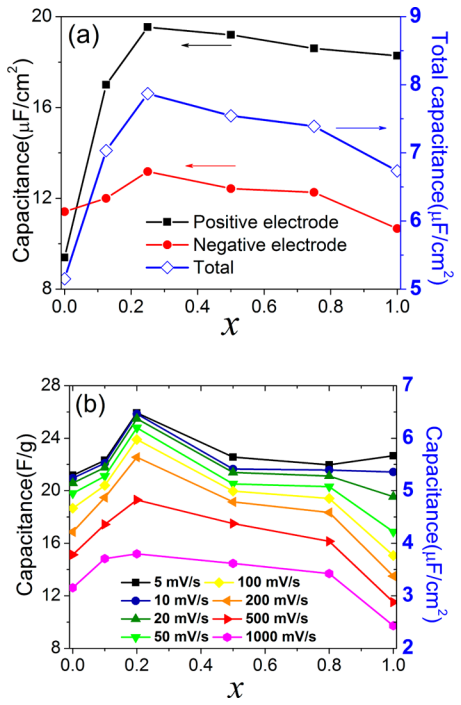

Figure 3. (a) Calculated integral capacitance for the positive, negative, and total electrodes when the operating potential window (OPW) is fixed as 3.0 V. (b) Experimental results for a symmetric supercapacitor operating at 3.0 V. The electrode capacitance is shown as a function of the concentration of the RTIL mixture for different scan rates.

of individual electrodes C_+ and C_-, and that of the entire cell, C_T. We calculate C_T from the integral capacitance corresponding to the negative and positive surfaces

$$1/C_T = 1/C_+ + 1/C_- \tag{9}$$

Figure 3a reveals that the integral capacitance for both the positive and negative electrodes first increases upon the addition of EMI-BF_4 until a peak is achieved at around x = 0.25, and a further increase of the BF_4 concentration reduces the capacitance. A similar trend is observed for the total integral capacitance. The maximum capacitance for C_T at x = 0.25 is ∼45% higher than that of pure EMI-TFSI and ∼15% higher than that of pure EMI-BF_4.

To study the concentration effect experimentally, we performed cyclic voltammetry (CV) measurements for onion-like carbon (OLC) electrodes in contact with EMI-BF_4-TFSI mixtures of different anion compositions. The cyclic voltammograms are given in the Supporting Information. Figure 3b shows the experimental results for the integral capacitance of the OLC-EDLC at different scan rates. As expected from the supercapacitor performance, the capacitance decreases with increasing the scan rate for all mixture concentrations. The concentration effect becomes more pronounced at slower scan rates, most likely because the system has more time to organize different ions and optimize the charge stored. Additionally, the

DOI: 10.1021/acsenergylett.6b00010
ACS Energy Lett. 2016, 1, 21−26

lower scan rates are better for comparing to the DFT calculations because the systems are closer to equilibrium. In all cases, the differential capacitance exhibits a volcano curve similar to that predicted by the theory, with the peak capacitance occurring at x = 0.2. At both higher and lower values of x, the capacitance decreases. Apparently, the theoretical predictions corroborate experimental results that the RTIL mixture with 20% EMI-BF_4 and 80% EMI-TFSI gives the best capacitive performance for the OLC electrodes. The device capacitance predicted by CDFT is 5−8 $\mu F/cm^2$ at equilibrium, which agrees well with the experimental results (~6 $\mu F/cm^2$) at low scan rates and is larger than the experimental value at high scan rates. As shown in Figure 3, the local maximum is about 20% higher than that expected from a linear interpolation of capacitance versus composition. Given the extremely simplified model we used for the EMI-TFSI/EMI-BF_4 mixtures, the quantitative agreement between the experiment and our CDFT results is quite remarkable.

Why is there a volcano-shaped trend in the capacitance versus electrolyte composition curves? To answer this question, we analyze the EDL structure for the pure RTILs and for the ionic mixtures. Figure 4 shows the density profiles of cations and anions for the pure RTILs and for the ionic mixture that yields the maximum overall capacitance (viz., x = 0, 0.25, and 1.0) near a positively charged surface (ψ − PZC = 1.5V). As expected, the EDL structure consists of a strong layer of counterions in contact with the surface (blue peak for TFSI and green peak for BF_4 in Figure 4). For pure EMI-TFSI (x = 0), the cations and anions have similar ion diameters. In this case, we observe alternating layers of cations and anions near the charged surface beyond about 10 times the ionic diameter. As indicated in our earlier work,[25] formation of the multiple ionic layers can be attributed to overscreening and the ionic excluded volume effects, and the layering structure cannot be captured by the Poisson−Boltzmann equation or lattice models. Adding small anions (BF_4^-) reduces the number of ionic layers near the surface and makes the layering structure less distinctive (Figure 4b). The concentration effect is also shown in the oscillatory integrated charge density (Figure S1). The oscillation of local electrical charge is reduced when the amount of small anions in the bulk is increased. The smaller ions reduce the thickness of ionic layers because of the smaller excluded volume and enhanced electrostatic interactions. In the ionic mixture, the electrode surface is preferentially in contact with small anions (BF_4^-), which decreases the effective thickness of EDLs[44−46] while increasing the overall ionic packing density.[46] As a result, adding smaller anions to pure EMI-TFSI raises the electrical charge at the electrode surface, thus resulting in a larger integral capacitance. Similarly, the total contact density of counterions for the RTIL mixture is larger than that of pure EMI-BF_4 (x = 1, Figure 4c), suggesting a better capacitive performance than pure EMI-BF_4.

The enhanced performance of the ionic liquid mixture is also evident by examining the density profiles of cations and anions near a negatively charged surface. As shown in Figure 5, the height and width of the first counterion peak is similar for all systems modeled at the negatively charged surface, because the counterion (EMI^+) is the same for the different electrolyte systems. This explains why the change of capacitance with mixture concentration at the negatively charged electrode is not as large as that of the positive electrode. Figure 5 also shows that the total contact density of counterions for the mixture is larger than that for pure RTILs, which explains the increased capacitance. However, for the pure RTIL with cations and anions of approximately the same size (0.5 and 0.6 nm, respectively), there is strong alternating cation/anion layering extending at least 4 nm from the surface, whereas the increasing addition of the smaller BF_4^- anions dampen this long-range oscillation, down to <2 nm for the pure EMI-BF_4. Previously,[47] we showed that the oscillating cation/anion layering in RTILs composed of equally sized cations and anions is also dampened in a similar way when the RTIL is diluted with polar solvents with dipole moments >~2 D but not for solvents with weaker polarity. In other words, we can manipulate the total capacitance and the extent of interfacial structuring of

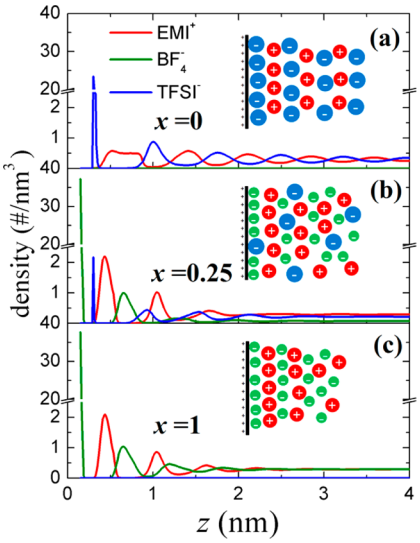

Figure 4. Distributions of cations (red line for EMI) and anions (green line for BF_4 and blue line for TFSI) in EDLs of pure and mixed RTILs near a positive surface with ψ − PZC = 1.5V: (a) x = 0, (b) x = 0.25, and (c) x = 1. Inserts are schematics of the EDL structures.

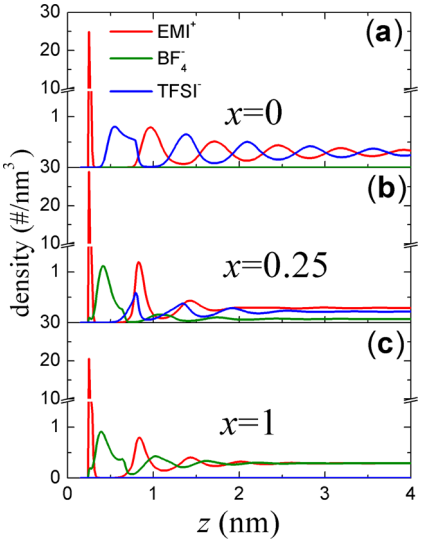

Figure 5. Distributions of cations (red line for EMI) and anions (green line for BF_4 and blue line for TFSI) in EDLs of pure and mixed RTILs near a negative surface with ψ − PZC = −1.5V.

DOI: 10.1021/acsenergylett.6b00010
ACS Energy Lett. 2016, 1, 21−26

electrode−electrolyte systems by controlling the cation−anion size disparity and/or by diluting with a polar solvent.

We can also understand the volcano-shaped trend of the capacitance versus the composition curve (Figure 3) by counting the number of counterions (e.g., ions of opposite charge to that of the electrode surface) per unit area in the region near the electrode where the charge overscreening dominates. For all systems considered in this work, the region of excess counterion density extends to about 0.8 nm from the electrode surface. Figure 6 shows that, at the same applied potential, the EDL contains more counterions when the TFSI anions are partially replaced by the BF_4 anions. The increased ionic density may be explained in terms of the smaller excluded volume of the BF_4^- anions. More counterions packing on and more co-ions leaving from this region in the presence of surface charge lead to a larger EDL capacitance.

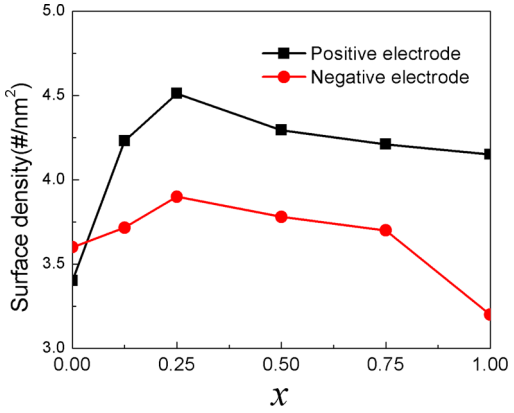

Figure 6. Number density of counterions near the positive (black) and negative (red) electrode.

In summary, we have investigated the influence of electrolyte composition for the EMI-TFSI/EMI-BF_4 mixtures on the integral capacitance and their EDL structures at the surface of carbon electrodes using theory and experiment. We find that the alternating layering structure can be dampened by the addition of smaller anions because of the reduced excluded volume effect and enhanced electrostatic interaction. With realistic parameters for the ionic liquids, the theory predicts an optimal composition of the RTIL mixtures that yields a maximum integral capacitance, according well with our experimental observations. In addition, there is a good agreement between the predicted and experimentally measured dependencies of integral capacitance on RTIL composition. Although this work is focused on a model system to represent ionic liquid mixtures near an onion-like carbon electrode, the theoretical and experimental procedures can potentially be extended to tuning RTIL mixtures for porous carbon electrodes. Considering the limited parameter space investigated in this work, we expect that the ion concentration effects will most likely be more complicated when the electrode structure and ion−surface interactions are fully taken into account. We hope that the promising features of the mixture effects will invite more systematic experimental validations and further theoretical exploration.

■ ASSOCIATED CONTENT

Supporting Information

The Supporting Information is available free of charge on the ACS Publications website at DOI: 10.1021/acsenergylett.6b00010.

Local charge density distributions predicted from the theory and cyclic voltammograms from experiments (PDF)

■ AUTHOR INFORMATION

Corresponding Author

*Tel: (951) 827-2413. E-mail: jwu@engr.ucr.edu.

Notes

The authors declare no competing financial interest.

■ ACKNOWLEDGMENTS

This research was sponsored by the Fluid Interface Reactions, Structures and Transport (FIRST) Center, an Energy Frontier Research Center funded by the U.S. Department of Energy, Office of Science, Office of Basic Energy Sciences. C.L. and H.L.L. acknowledge the financial support by the National Natural Science Foundation of China (91334203, 21376074) and the 111 Project of China (B08021). C.L. is also grateful to the Chinese Scholarship Council for the visiting fellowship. The numerical calculations were performed at the National Energy Research Scientific Computing Center (NERSC).

■ REFERENCES

(1) Simon, P.; Gogotsi, Y. Capacitive energy storage in nanostructured carbon−electrolyte systems. *Acc. Chem. Res.* **2013**, *46*, 1094−1103.

(2) Burt, R.; Birkett, G.; Zhao, X. A review of molecular modelling of electric double layer capacitors. *Phys. Chem. Chem. Phys.* **2014**, *16*, 6519−6538.

(3) Zhong, C.; Deng, Y.; Hu, W.; Qiao, J.; Zhang, L.; Zhang, J. A review of electrolyte materials and compositions for electrochemical supercapacitors. *Chem. Soc. Rev.* **2015**, *44*, 7484−7539.

(4) Jiang, D.-e.; Wu, J. Microscopic insights into the electrochemical behavior of nonaqueous electrolytes in electric double-layer capacitors. *J. Phys. Chem. Lett.* **2013**, *4*, 1260−1267.

(5) Shao, Y.; El-Kady, M. F.; Wang, L. J.; Zhang, Q.; Li, Y.; Wang, H.; Mousavi, M. F.; Kaner, R. B. Graphene-based materials for flexible supercapacitors. *Chem. Soc. Rev.* **2015**, *44*, 3639−3665.

(6) Fedorov, M. V.; Kornyshev, A. A. Ionic liquids at electrified interfaces. *Chem. Rev.* **2014**, *114*, 2978−3036.

(7) Frackowiak, E.; Abbas, Q.; Béguin, F. Carbon/carbon supercapacitors. *J. Energy Chem.* **2013**, *22*, 226−240.

(8) Pilon, L.; Wang, H.; d'Entremont, A. Recent advances in continuum modeling of interfacial and transport phenomena in electric double layer capacitors. *J. Electrochem. Soc.* **2015**, *162*, A5158−A5178.

(9) Kornyshev, A. A. Double-layer in ionic liquids: paradigm change? *J. Phys. Chem. B* **2007**, *111*, 5545−5557.

(10) Fedorov, M. V.; Kornyshev, A. A. Towards understanding the structure and capacitance of electrical double layer in ionic liquids. *Electrochim. Acta* **2008**, *53*, 6835−6840.

(11) Wang, G.; Zhang, L.; Zhang, J. A review of electrode materials for electrochemical supercapacitors. *Chem. Soc. Rev.* **2012**, *41*, 797−828.

(12) Liu, R.; Duay, J.; Lee, S. B. Heterogeneous nanostructured electrode materials for electrochemical energy storage. *Chem. Commun.* **2011**, *47*, 1384−1404.

(13) Simon, P.; Gogotsi, Y. Materials for electrochemical capacitors. *Nat. Mater.* **2008**, *7*, 845−854.

(14) Lin, R.; Huang, P.; Ségalini, J.; Largeot, C.; Taberna, P. L.; Chmiola, J.; Gogotsi, Y.; Simon, P. Solvent effect on the ion

DOI: 10.1021/acsenergylett.6b00010
ACS Energy Lett. 2016, 1, 21−26

adsorption from ionic liquid electrolyte into subnanometer carbon pores. *Electrochim. Acta* **2009**, *54*, 7025−7032.
(15) Vatamanu, J.; Hu, Z.; Bedrov, D.; Perez, C.; Gogotsi, Y. Increasing energy storage in electrochemical capacitors with ionic liquid electrolytes and nanostructured carbon electrodes. *J. Phys. Chem. Lett.* **2013**, *4*, 2829−2837.
(16) Seddon, K. R. Ionic liquids for clean technology. *J. Chem. Technol. Biotechnol.* **1997**, *68*, 351−356.
(17) Weng, Z.; Li, F.; Wang, D. W.; Wen, L.; Cheng, H. M. Controlled electrochemical charge injection to maximize the energy density of supercapacitors. *Angew. Chem.* **2013**, *125*, 3810−3813.
(18) Vaquero, S.; Palma, J.; Anderson, M.; Marcilla, R. Improving performance of electric double layer capacitors with a mixture of ionic liquid and acetonitrile as the electrolyte by using mass-balancing carbon electrodes. *J. Electrochem. Soc.* **2013**, *160*, A2064−A2069.
(19) Khomenko, V.; Raymundo-Piñero, E.; Béguin, F. A new type of high energy asymmetric capacitor with nanoporous carbon electrodes in aqueous electrolyte. *J. Power Sources* **2010**, *195*, 4234−4241.
(20) Van Aken, K. L.; Beidaghi, M.; Gogotsi, Y. Formulation of ionic-liquid electrolyte to expand the voltage window of supercapacitors. *Angew. Chem., Int. Ed.* **2015**, *54*, 4806−4809.
(21) Hayes, R.; Warr, G. G.; Atkin, R. Structure and nanostructure in ionic liquids. *Chem. Rev.* **2015**, *115*, 6357−6426.
(22) Forsman, J.; Woodward, C. E.; Szparaga, R. Classical density functional theory of ionic solutions. In *Computational Electrostatics for Biological Applications*; Springer: New York, 2015; pp 17−38.
(23) Ma, K.; Woodward, C. E.; Forsman, J. Classical density functional study on interfacial structure and differential capacitance of ionic liquids near charged surfaces. *J. Phys. Chem. C* **2014**, *118*, 15825−15834.
(24) Bazant, M. Z.; Storey, B. D.; Kornyshev, A. A. Double layer in ionic liquids: Overscreening versus crowding. *Phys. Rev. Lett.* **2011**, *106*, 046102.
(25) Wu, J.; Jiang, T.; Jiang, D.-e.; Jin, Z.; Henderson, D. A classical density functional theory for interfacial layering of ionic liquids. *Soft Matter* **2011**, *7*, 11222−11231.
(26) Mezger, M.; Schröder, H.; Reichert, H.; Schramm, S.; Okasinski, J. S.; Schöder, S.; Honkimäki, V.; Deutsch, M.; Ocko, B. M.; Ralston, J.; et al. Molecular layering of fluorinated ionic liquids at a charged sapphire (0001) surface. *Science* **2008**, *322*, 424−428.
(27) Feng, G.; Huang, J.; Sumpter, B. G.; Meunier, V.; Qiao, R. Structure and dynamics of electrical double layers in organic electrolytes. *Phys. Chem. Chem. Phys.* **2010**, *12*, 5468−5479.
(28) Feng, G.; Jiang, X.; Qiao, R.; Kornyshev, A. A. Water in ionic liquids at electrified interfaces: The anatomy of electrosorption. *ACS Nano* **2014**, *8*, 11685−11694.
(29) Zhan, C.; Neal, J.; Wu, J.; Jiang, D.-e. Quantum effects on the capacitance of graphene-based electrodes. *J. Phys. Chem. C* **2015**, *119*, 22297−22303.
(30) Hu, Z.; Vatamanu, J.; Borodin, O.; Bedrov, D. A comparative study of alkylimidazolium room temperature ionic liquids with FSI and TFSI anions near charged electrodes. *Electrochim. Acta* **2014**, *145*, 40−52.
(31) Vatamanu, J.; Vatamanu, M.; Bedrov, D. Non-Faradaic energy storage by room temperature ionic liquids in nanoporous electrodes. *ACS Nano* **2015**, *9*, 5999−6017.
(32) Costa, R.; Pereira, C. M.; Silva, A. F. Structural ordering transitions in ionic liquids mixtures. *Electrochem. Commun.* **2015**, *57*, 10−13.
(33) dos Santos, D. J.; Cordeiro, M. N. D. Effect of replacing [NTf2] by [PF6] anion on the [BMIm][NTf2] ionic liquid confined by gold. *Mol. Simul.* **2015**, *41*, 455−462.
(34) Siimenson, C.; Siinor, L.; Lust, K.; Lust, E. Electrochemical characterization of iodide ions adsorption kinetics at bi (111) electrode from three-component ionic liquids mixtures. *ECS Electrochem. Lett.* **2015**, *4*, H62−H65.
(35) Lall-Ramnarine, S.; Suarez, S.; Zmich, N.; Ewko, D.; Ramati, S.; Cuffari, D.; Sahin, M.; Adam, Y.; Rosario, E.; Paterno, D. Binary ionic liquid mixtures for supercapacitor applications. *ECS Trans.* **2014**, *64*, 57−69.
(36) Jiang, D.-e.; Meng, D.; Wu, J. Density functional theory for differential capacitance of planar electric double layers in ionic liquids. *Chem. Phys. Lett.* **2011**, *504*, 153−158.
(37) *Materials Studio*, 7.0 ed.; Accelrys Software Inc.: San Diego, CA, 2013.
(38) Jiang, D.-e.; Jin, Z.; Wu, J. Oscillation of capacitance inside nanopores. *Nano Lett.* **2011**, *11*, 5373−5377.
(39) Li, S.; Feng, G.; Fulvio, P. F.; Hillesheim, P. C.; Liao, C.; Dai, S.; Cummings, P. T. Molecular dynamics simulation study of the capacitive performance of a binary mixture of ionic liquids near an onion-like carbon electrode. *J. Phys. Chem. Lett.* **2012**, *3*, 2465−2469.
(40) McDonough, J. K.; Gogotsi, Y. Carbon onions: Synthesis and electrochemical applications. *Electrochem. Soc. Interface* **2013**, *22*, 61−65.
(41) Feng, G.; Jiang, D.-e.; Cummings, P. T. Curvature effect on the capacitance of electric double layers at ionic liquid/onion-like carbon interfaces. *J. Chem. Theory Comput.* **2012**, *8*, 1058−1063.
(42) Wu, J.; Li, Z. Density-functional theory for complex fluids. *Annu. Rev. Phys. Chem.* **2007**, *58*, 85−112.
(43) Van Aken, K. L.; McDonough, J. K.; Li, S.; Feng, G.; Chathoth, S. M.; Mamontov, E.; Fulvio, P. F.; Cummings, P. T.; Dai, S.; Gogotsi, Y. Effect of cation on diffusion coefficient of ionic liquids at onion-like carbon electrodes. *J. Phys.: Condens. Matter* **2014**, *26*, 284104.
(44) Feng, G.; Zhang, J.; Qiao, R. Microstructure and capacitance of the electrical double layers at the interface of ionic liquids and planar electrodes. *J. Phys. Chem. C* **2009**, *113*, 4549−4559.
(45) Feng, G.; Qiao, R.; Huang, J.; Dai, S.; Sumpter, B. G.; Meunier, V. The importance of ion size and electrode curvature on electrical double layers in ionic liquids. *Phys. Chem. Chem. Phys.* **2011**, *13*, 1152−1161.
(46) Georgi, N.; Kornyshev, A. A.; Fedorov, M. V. The anatomy of the double layer and capacitance in ionic liquids with anisotropic ions: Electrostriction vs. lattice saturation. *J. Electroanal. Chem.* **2010**, *649*, 261−267.
(47) Jiang, D.-e.; Wu, J. Unusual effects of solvent polarity on capacitance for organic electrolytes in a nanoporous electrode. *Nanoscale* **2014**, *6*, 5545−5550.

DOI: 10.1021/acsenergylett.6b00010
ACS Energy Lett. 2016, 1, 21−26